

Original Article

Mutant SOD1 microglia-generated nitroxidative stress promotes toxicity to human fetal neural stem cell-derived motor neurons through direct damage and noxious interactions with astrocytes

Jason R. Thonhoff¹, Junling Gao¹, Tiffany J. Dunn¹, Luis Ojeda², Ping Wu¹

¹Department of Neuroscience and Cell Biology, ²Department of Biochemistry and Molecular Biology, University of Texas Medical Branch, Galveston, Texas 77555, USA

Received August 10, 2011; accepted August 18, 2011; Epub August 19, 2011; published January 1, 2012

Abstract: Amyotrophic lateral sclerosis (ALS) is a devastating motor neuron disease. Human neural stem cells (hNSCs) may have the potential to replace lost motor neurons. The therapeutic efficacy of stem cell therapy depends greatly on the survival of grafted stem cell-derived motor neurons in the microenvironment of the spinal cord in ALS. After transplantation of hNSCs into the spinal cords of transgenic ALS rats, morphological analysis reveals that grafted hNSCs differentiate into motor neurons. However, hNSCs degenerate and show signs of nitroxidative damage at the disease end-stage. Using an *in vitro* coculture system, we systematically assess interactions between microglia and astroglia derived from both nontransgenic rats and transgenic rats expressing human mutant SOD1^{G93A} before and after symptomatic disease onset, and determine the effects of such microglia-astroglia interactions on the survival of hNSC-derived motor neurons. We found that ALS microglia, specifically isolated after symptomatic disease onset, are directly toxic to hNSC-derived motor neurons. Furthermore, nontransgenic astrocytes not only lose their protective role in hNSC-derived motor neuron survival *in vitro*, but also exhibit toxic features when cocultured with mutant SOD1^{G93A} microglia. Using inhibitors of inducible nitric oxide synthase and NADPH oxidase, we show that microglia-generated nitric oxide and superoxide partially contribute to motor neuron loss and astrocyte dysfunction in this coculture paradigm. In summary, reactive oxygen/nitrogen species released from overactivated microglia in ALS directly eliminate human neural stem cell-derived motor neurons and reduce the neuroprotective capacities of astrocytes.

Keywords: Amyotrophic lateral sclerosis, microglia, astroglia, motor neuron, transplantation, oxidative stress

Introduction

Amyotrophic lateral sclerosis (ALS) is the most common adult motor neuron disease and 1-2% of patients have familial ALS due to mutations in superoxide dismutase 1 (SOD1) [1]. Current evidence, accumulated from transgenic rodent models expressing human mutant SOD1, indicates that mutant SOD1 expression within motor neurons and other unidentified cell types determines the rate of disease onset [2,3]. Disease progression after onset, on the other hand, is hastened by the activation and dysfunction of surrounding mutant SOD1-expressing microglia and astrocytes [2,4-6]. Microgliosis and astrogliosis in areas of motor neuron degeneration are pathological hallmarks of ALS [7,8]. Oxidative

stress beyond endogenous antioxidant capabilities is also observed in ALS. Evidence of oxidative damage, including increased protein carbonylation [9], protein nitration [10] and lipid peroxidation [11] has been described in both ALS patients and transgenic ALS animal models.

ALS is often diagnosed very late in the disease course after numerous motor neurons have already been lost. Thus, in order to reinnervate muscle tissue and repair muscle function, motor neurons will need to be replaced. Many stem cell therapies have previously been tested in transgenic ALS rodent models [12-14]. However, the slight benefits shown in some studies, including our experiment in which lifespan was prolonged by 17 days (unpublished observa-

tion), were most likely due to the neuroprotection of endogenous motor neurons rather than motor neuron replacement. Advances in techniques for motor neuron differentiation from stem cells [14] allow specifically for the exploration of motor neuron cell-replacement therapy in transgenic ALS models. Further, several recent studies have shown that stem cell-derived motor neurons are susceptible to damage in the neural microenvironment of transgenic ALS animals through organotypic slice cultures and cocultures with primary astrocytes [15-19]. Thus, the hostile spinal microenvironment in ALS may be detrimental to the survival and maturation of transplanted stem cell-derived motor neurons.

Here, we sought to determine whether the grafted cells could differentiate into motor neurons and survive within the toxic spinal microenvironment *in vivo*. Furthermore, it is unclear how microglia and astrocytes interact with each other to create such a toxic environment, and to what extent nitroxidative stress is involved in motor neuron toxicity. Thus, we provide evidence that primary microglia isolated from transgenic ALS rats after symptomatic disease onset, through generating reactive oxygen/nitrogen species, specifically affect the survival of hNSC-derived motor neurons by direct nitroxidative damage and detrimental interactions with normally neuroprotective astrocytes.

Materials and methods

Human NSC culture

The primary K048 line of human cortical NSCs was cultured as neurospheres according to our previous description [20,21]. Growth media contained a basic media consisting of DMEM (high glucose, L-glutamine)/Hams-F12 (3:1) (Invitrogen/GIBCO, Carlsbad, CA), 15 mM HEPES (Sigma, St. Louis, MO), 1.5% D-glucose (Sigma), 67 I.U./ml/67 µg/ml penicillin/streptomycin (Cellgro, Herndon, VA) and 2 mM L-glutamine (Sigma). The basic media was supplemented with N2, including 25 µg/ml bovine insulin (Sigma), 100 µg/ml human transferrin (Sigma), 100 µM putrescine (Sigma), 20 nM progesterone (Sigma) and 30 nM sodium selenite (Sigma) [22]. Growth media was further supplemented with 20 ng/ml recombinant human epidermal growth factor (EGF) (R&D Systems, Minneapolis, MN), 20 ng/ml recombinant human basic fibroblast growth factor (bFGF)

(R&D Systems), 5 µg/ml heparin (Sigma) and 10 ng/ml recombinant human leukemia inhibitory factor (LIF) (Chemicon, Temecula, CA).

Human NSC priming and differentiation

Priming was performed according to our previous description [21,23]. Three to four days after passage (passages 15-35), approximately 2-4 million hNSCs in neurospheres were seeded in 25 cm² flasks with the basic media and N2 described above and primed with 10 ng/ml bFGF, 2.5 µg/ml heparin and 1 µg/ml laminin (LMN, Invitrogen) for 4 days. Primed cells were then cultured in differentiation medium, which consisted of the basic medium supplemented with 20 µl/ml B27 (GIBCO). After 6-7 days, differentiated hNSCs were dissociated according to our previous description [24,25] and used in all coculture experiments described below.

Transgenic ALS rats

Male hemizygous NTac:SD-TgN(SOD1G93A) L26H rats (Taconic, Hudson, NY) [26] were crossed with normal female Wistar rats (Charles River Laboratories, Wilmington, MA) and genotyped by PCR analyses with human mutant SOD1 primers according to our previous description [27]. The animal protocol was approved by the Institutional Animal Care and Use Committee (IACUC) at the University of Texas Medical Branch. Male and female transgenic ALS rats were used in all transplantation (total of 28 rats) and primary glia extraction experiments. Control nontransgenic rats were always sex-matched and age-matched, and were littermates whenever possible.

Symptomatic disease onset and disease progression post-disease onset were assessed using a modified 5-point motor score system according to our previous description [27]. A score of 5 represented normal movement whereas a score of 0 (disease end-stage) represented the absence of righting reflexes within a 30-second time period, at which time the rats were euthanized. Lifespan was determined by the age at the disease end-stage. Disease onset was determined when the rats first showed abnormal gait signs, which denoted a motor score of 4.

Human NSC transplantation

Human NSCs were cultured, transduced by a recombinant adeno-associated viral vector con-

taining the enhanced green fluorescent protein gene, AAVegfp, and transplanted according to our previous description [23-25]. At 4 months of age, transgenic or nontransgenic rats received stereotactic transplantation of hNSCs into the ventral horns of spinal cords bilaterally at L4-5 and 1×10^5 hNSCs were injected per site (2 injection sites). All transplanted rats were immunosuppressed with NEORAL cyclosporine (Novartis Pharmaceuticals, East Hanover, NJ) at 100 $\mu\text{g}/\text{ml}$ in drinking water beginning 3 days prior to transplantation and then throughout the lifespan of the animals. All surgery protocols were performed under aseptic conditions in compliance with the NIH Guide for the Care and Use of Laboratory Animals.

Primary astrocyte isolation

Primary spinal cord astrocytes were generated from transgenic ALS rats and nontransgenic littermates according to previously described methods [28] with modifications [29]. Lumbar spinal cord sections (1 cm) were pooled from three ALS rats after symptomatic disease onset or 1 month of age and nontransgenic control rats. Astrocytes were cultured in glia growth medium (GGM) consisting of DMEM/F12 (3:1) supplemented with 10% fetal bovine serum (FBS, GIBCO), 15 mM HEPES, 1.5% D-glucose, 67 I.U./ml penicillin and 67 $\mu\text{g}/\text{ml}$ streptomycin. At confluence, astrocytes were dissociated by adding 0.25% trypsin-EDTA (GIBCO) in dPBS (1:4 dilution) for 20 minutes according to a previously described method [30] with modifications. Many cells remained attached (presumably microglia), but floating cells were collected and plated in GGM in new flasks at $0.5\text{-}1 \times 10^6$ cells/25 cm^2 . Cytosine arabinofuranoside (10 μM , Sigma) was added to the GGM overnight to inhibit any rapidly dividing cells (presumably fibroblasts). Cells from passage 2-5 were used for experiments.

Primary microglia isolation

Pure microglia were isolated from combined whole brain and spinal cord tissue using a density gradient centrifugation method in Percoll solutions [31] with slight modifications. Briefly, brains and spinal cords were pooled from three transgenic ALS rats after symptomatic disease onset or 1 month of age and nontransgenic control rats. After isolation by density gradient centrifugation according to the method described

by Frank and colleagues [34], microglia were cultured in media containing half GGM and half conditioned medium from 3-day post-passage L929 fibroblast cell culture, which was collected and stored at -80°C . L929 fibroblasts (ATCC, Manassas, VA) secrete macrophage-colony stimulating factor (M-CSF) [32], which is a growth factor for microglia [33]. L929 fibroblasts were cultured in DMEM with 5% FBS. Isolated microglia were immediately plated for coculture experiments. The yield of microglia was approximately $1\text{-}3 \times 10^5$ per rat, with the purity of 98% confirmed by immunofluorescent analyses using the microglial marker Iba1. Other microglial markers such as CD11b and CD68 were also used to further verify the cell phenotype.

Cocultures of hNSCs and glia

For all coculture experiments, cell numbers were approximately 150,000 differentiated hNSCs, 50,000 microglia and 100,000 astrocytes. German glass coverslips (Carolina Biological Supply, Burlington, NC) in 24-well plates were pre-treated with 0.01% poly-D-lysine and 1 $\mu\text{g}/\text{cm}^2$ LMN. In experiments with microglia in direct contact coculture with hNSCs, microglia were plated on PDL/LMN-coated coverslips immediately after isolation and cultured for four days to allow for recovery. Differentiated hNSCs were plated on top of microglia in B27 medium overnight. B27 medium was then replaced with basic medium supplemented with N2 (N2 medium) containing either vehicle (DMSO or dH_2O), apocynin (Sigma), N6-(1-iminoethyl)-L-lysine dihydrochloride (L-NIL, Cayman Chemical, Ann Arbor, MI), Urate (Sigma), Carboxy-PTIO (Calbiochem, Gibbstown, NJ), MK 0524 (Cayman Chemical) or SOD (Sigma). In experiments with microglia and hNSCs in non-contact coculture, microglia were plated in 0.4 μm polyester membrane transwells (Corning, Corning, NY) and cultured for 4 days. Differentiated hNSCs were plated on PDL/LMN-coated coverslips in a 24-well plate in B27 medium overnight. Cocultures were then initiated in N2 medium. Non-contact cocultures of hNSCs and astrocytes were performed in the same manner as microglia except astrocytes were plated in 3.0 μm polyester membrane transwells (Corning) and allowed to recover in GGM overnight prior to coculture in N2 medium. If glutathione depletion was required, astrocytes were incubated in N2 medium with vehicle

(DMSO) or ethacrynic acid (Sigma) for 24 hours prior to initiating the coculture. In experiments in which microglia and astrocytes were cocultured in direct contact with each other, microglia were first plated in 0.4 μm transwells or on PDL/LMN-coated coverslips and allowed to recover for 4 days. Astrocytes were plated on top of microglia in GGM overnight and then changed to N2 medium. Half the N2 medium with appropriate drug concentrations was changed after 3 days in all experiments. Cells on coverslips were fixed in 4% paraformaldehyde for immunofluorescent analyses after 7 days in coculture. In a subset of experiments without primary glia, differentiated hNSCs were directly treated with increasing doses (1 nM – 10 μM) of prostaglandin D2 (PGD2, Cayman Chemical) or vehicle (DMSO), in N2 medium for 7 days before fixation.

Immunofluorescent staining

Immunocytofluorescent staining was performed according to our previous descriptions [20,21]. Primary antibodies, including monoclonal anti-Hb9 (1:100, Developmental Studies Hybridoma Bank), rabbit polyclonal anti-microtubule associated protein 2 (MAP2, 1:500, Chemicon), rabbit polyclonal anti-Iba1 (1:500, Wako, Richmond, VA), monoclonal anti-CD68 (1:100, AbD Serotec, Raleigh, NC) and monoclonal anti-CD11b (1:100, Chemicon), as well as Alexa fluorophore-conjugated secondary antibodies (Molecular Probes, Carlsbad, CA), 568 goat anti-mouse (1:400) and 488 goat anti-rabbit (1:400), were utilized. Images were acquired with a Nikon 80i epifluorescent microscope using NIS-Elements imaging software.

Immunohistofluorescent staining was performed according to our previous descriptions [23,24]. For immunostaining with 4-HNE, sections were first exposed to sodium borohydride (50 mM) and MOPS buffer (100 mM), pH 8.0, for 10 minutes prior to serum blocking. Goat polyclonal anti-ChAT (1:100, Chemicon), rabbit polyclonal anti-GFAP (1:1,000, Chemicon), rabbit polyclonal anti-Iba1 (1:500, Wako, Richmond, VA), rabbit polyclonal anti-nitrotyrosine (7.5 $\mu\text{g}/\text{ml}$) (Upstate Cell Signaling Solutions, Lake Placid, NY) and rabbit polyclonal anti-4-HNE (1:200, Calbiochem) primary antibodies and alexa fluorophore-conjugated secondary antibodies (Molecular Probes) were used. Images were acquired with a Nikon D-Eclipse C1

Laser Scanning Confocal microscope.

Immunocytochemistry

For immunocytochemistry, cells were fixed in 4% paraformaldehyde and post-fixed with 0.3% H_2O_2 in methanol. The Vectastain ABC kit (Vector Laboratories, Burlingame, CA) was used according to manufacturer's instructions. Primary rabbit polyclonal anti-4-HNE (1:3,000, Calbiochem) and goat anti-rabbit IgG (1:200, Vector Laboratories) were used. Cells were incubated with 0.025% diaminobenzidine tetrahydrochloride (DAB, Sigma) and 0.01% H_2O_2 .

For immunohistochemistry, spinal cord sections were deparaffinized in xylene and rehydrated through serial concentrations of ethanol. Following antigen retrieval in microwave (2 min, 700 watt), sections were post-fixed with 0.3% H_2O_2 in methanol and then blocked with 1.5% NGS for 30 minutes at room temperature. Primary antibodies included rabbit polyclonal anti-nitrotyrosine (5 $\mu\text{g}/\text{ml}$, Upstate Cell Signaling Solutions) and rabbit polyclonal anti-4-HNE (1:200, Calbiochem). Horseradish peroxidase-conjugated goat anti-rabbit IgG (1:200) was used as the secondary antibody (Upstate Cell Signaling Solutions). The Vectastain ABC kit (Vector Laboratories) was applied according to the manufacturer's instruction.

TUNEL staining

Cells were fixed in 4% paraformaldehyde. For TdT-mediated dUTP nick end labeling (TUNEL) staining, the TACS® 2 Tdt-Fluor *In Situ* Apoptosis Detection Kit (Trevigen, Gaithersburg, MD) was used according to the manufacturer's instructions. Images were acquired with a Nikon 80i epifluorescent microscope using NIS-Elements imaging software.

Superoxide assay

Superoxide release from glia was determined by the reduction of the WST-1 reagent (Dojindo Laboratories, Rockville, MD) according to standard methods [34,35]. WST-1 (300 μM) and catalase (10 U/ml, Sigma) in Hanks' Balanced Salt Solution (HBSS, Cellgro) were added to the samples. Phorbol myristate acetate (PMA, 800 nM, Calbiochem) was then added to initiate the reaction. After 2-hour incubation, the absorbance was measured at 450 nm on an ELx800uv

Universal Microplate Reader (Biotek Instruments, Inc., Winooski, VT).

Nitric oxide assay

Total nitric oxide production was determined through the assessment of total nitrate and nitrite in the culture medium using the Nitrate-Nitrite Assay Kit (Cayman Chemical) according to the manufacturer's instructions. The absorbance was measured at 540 nm on an ELx800uv Universal Microplate Reader.

Prostaglandin D2 assay

PGD2 in the culture medium was quantified by an ELISA assay using the Prostaglandin D2 EIA Kit (Cayman Chemical) according to the manufacturer's protocol. The absorbance was measured at 405 nm on an ELx800uv Universal Microplate Reader and PGD2 concentration was calculated.

Statistical analyses

Statistical analyses were done using GraphPad Prism Version 4 software (GraphPad Software, San Diego, CA). The Student's *t*-test was used when comparing two groups. A one-way ANOVA was used for comparing multiple groups. Post-hoc Tukey and Dunnett tests were used on some sets of data. A *p* value less than 0.05 was considered statistically significant. All data were expressed as means \pm S.E.M.

Results

Transplanted hNSCs differentiate into cholinergic cells and undergo nitroxidative damage in ALS spinal cords

In this context, "ALS" rats or cells refer to those expressing transgenic mutant SOD1 and "normal" refers to nontransgenic matches. Morphological analyses were performed at the lumbar grafting sites to determine the fate of transplanted hNSCs. A total of 28 ALS rats received hNSC transplants at L4-5 bilaterally at age 4 months and were then euthanized at the disease end-stage. The spinal cord tissues were subjected to various immunofluorescent or immunohistochemical analyses. Normal rats were simultaneously transplanted with hNSCs and sacrificed similarly. The age at transplantation was prior to symptomatic disease onset

(approximately 167 days), but near an early disease stage characterized by motor weakness and weight loss as previously described [27]. The time point was chosen not only for its clinical relevance, but also for evaluating the potential for reinnervation of muscle targets, since it takes approximately 3 months for axons of grafted hNSC-derived motor neurons to reach the target gastrocnemius muscle in wild-type adult rats as we reported previously [24].

Grafted GFP⁺-hNSCs in normal cord expressed choline acetyltransferase (ChAT), which indicated that hNSCs become motor neurons (**Figure 1A**). Many GFP⁺/ChAT⁺ cells found in the spinal cord of ALS rats at the disease end-stage showed a degenerated morphology (punctuated GFP labeling, smaller size, lack of elongated neurites, **Figure 1B** and **1C-right** image) compared to those observed in the normal cord (smooth GFP filling, large in size and many GFP-filled neurites, **Figure 1A** and **1C-left** image). Several transplanted cells lost their typical motor neuron morphology (arrows in **Figure 1B**). Accordingly, GFP⁺/ChAT⁺ cells found in the ALS spinal cords exhibited a significantly smaller average maximum soma diameter (33% decrease) than those grafted into the normal spinal cords (**Figure 1C**). Based on our previous studies, the survival rate of grafted cells in normal rat spinal cord is approximately 5% [23]. However, the survival rate within the spinal cord of ALS rats has not been thoroughly explored, since the deteriorating morphology of the cells prevented an accurate estimation. Although grafted GFP⁺/ChAT⁺ cells showed degenerative changes in ALS spinal cords, a few GFP⁺ fibers had extended into the ventral white matter (**Figure 1D**) and down the L5 ventral root (**Figure 1E**), which indicated that some hNSC-derived motor neurons have the potential to reinnervate distal muscle fibers if they survived long enough in ALS rats.

Similar to the previous findings, microgliosis, indicated by Iba1 (pan-microglia marker) (**Figure 2A, B**), and astrogliosis, shown by intense GFAP immunoreactivity (**Figure 2C, D**), were apparent within the ventral horns of ALS rat spinal cords (**Figure 2A, C**), but not normal cords (**Figure 2B, D**). Microgliosis and astrogliosis in the ventral horns of ALS cords were accompanied by increased 3-nitrotyrosine (NT) (**Figure 2E**), a marker of protein nitration, and the 4-hydroxynonenal adduct (HNE) (**Figure 2G**), a

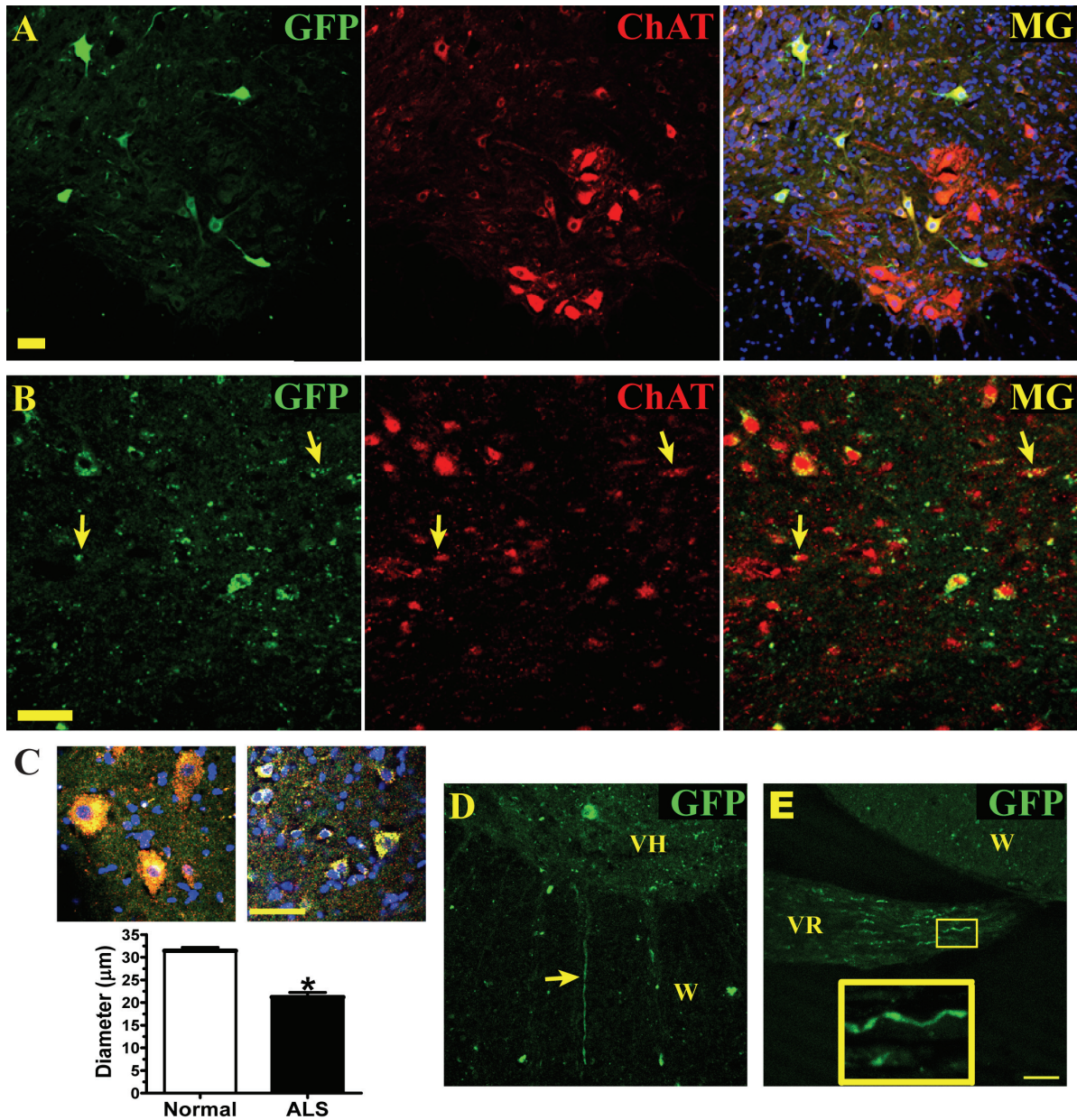


Figure 1. Human NSCs degenerate in the spinal cord of ALS rats at the end-stage. **A**, Normal spinal cord, hNSCs (labeled with green fluorescent protein, GFP) express choline acetyltransferase (ChAT), and merged image (MG) with DAPI shown in blue. **B**, ALS cord, hNSCs (GFP) express ChAT. Arrow, deteriorating GFP⁺/ChAT⁺ fragments. **C**, Higher magnification images of hNSCs (GFP in green) colabeled with ChAT (red) and DAPI (blue) in normal (left) and ALS (right) spinal cords. Average maximum soma diameter of GFP⁺/ChAT⁺ derived from hNSCs in either normal or ALS spinal cords, n = 3 rats/group. Data expressed as mean ± SEM. *p < 0.05, significantly different from normal group by Student's *t*-test. **D**, GFP⁺ fiber exiting ventral horn (VH) into the white matter (W) in ALS cord. **E**, GFP⁺ fibers, with magnified section (yellow box), coursing through the L5 ventral root (VR) from ALS spinal cord. **A-B** and **D-E**, scale bars = 50 μm.

marker of lipid peroxidation, compared to those in normal cords (**Figure 2F, H**). In correlation with these results, many grafted GFP⁺ hNSCs that were severely degenerated (arrowheads in

Figure 2I-J) in the ventral horn had incurred nitroxidative damage by the disease end-stage as shown by co-immunolabeling with NT (**Figure 2I**) and HNE (**Figure 2J**).

Glial interactions and toxicity to motoneurons

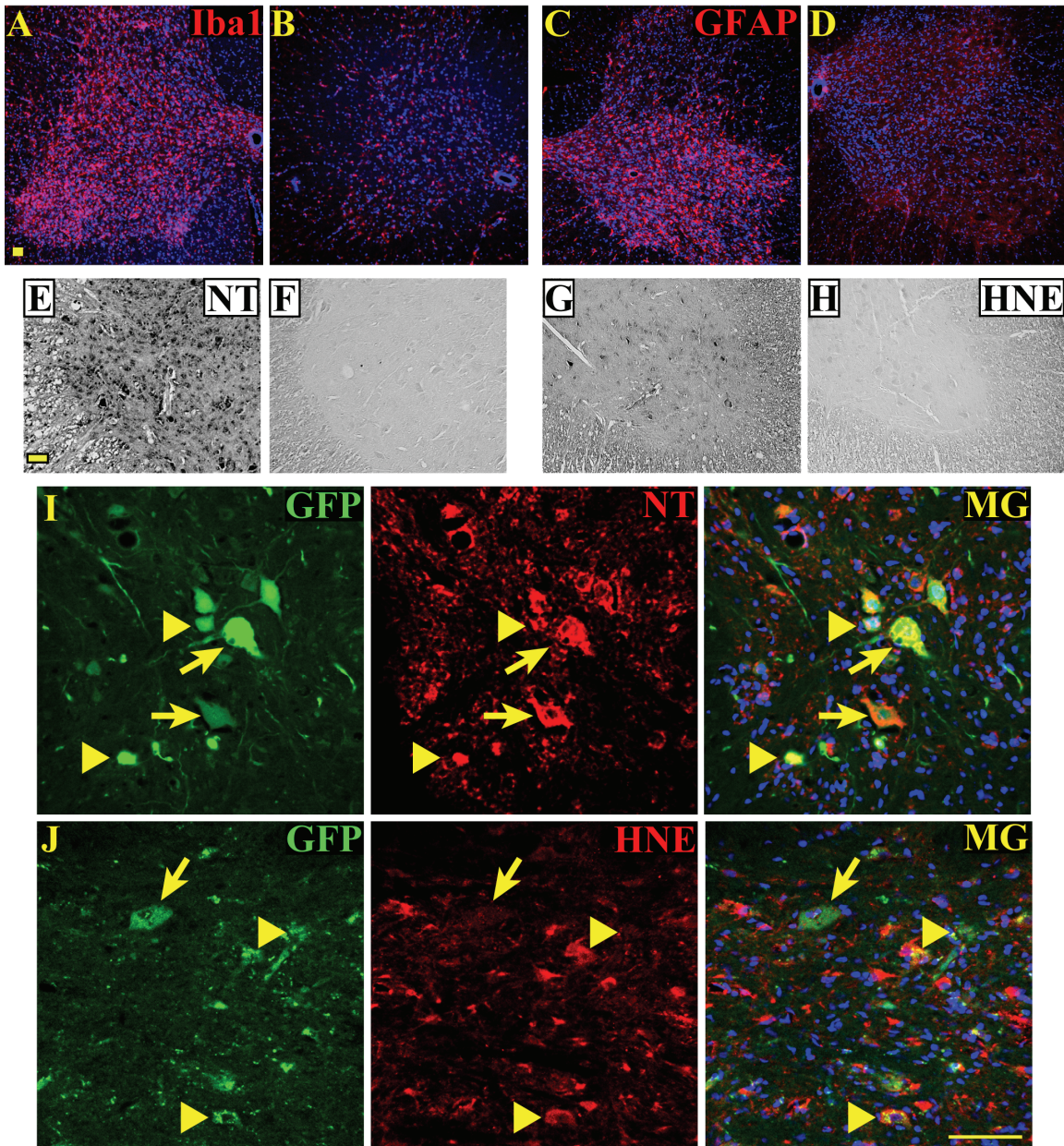


Figure 2. Human NSCs exhibit nitroxidative damage in the spinal cord of ALS rats at the end-stage. **A**, Microgliosis, shown by Iba1 staining (pan-microglia marker, red) in ALS spinal cord. **B**, Normal cord, resident microglia with low levels of Iba1 staining. **C**, ALS cord, astrogliosis (intense GFAP, astroglia marker, red) in ventral horn. **D**, Normal cord, minimal GFAP staining. **E**, ALS cord, increased protein nitration shown by 3-nitrotyrosine staining (NT, black) in ventral horn. **F**, Normal cord, no observable protein nitration. **G**, ALS cord, increased lipid peroxidation shown by 4-hydroxynonenal staining (HNE, black) in ventral horn. **H**, Normal cord, no observable lipid peroxidation. **I**, ALS spinal cord, hNSCs (GFP, green) exhibit NT immuno-labeling (arrows and arrowheads). Severely degenerated hNSCs labeled with NT (arrowheads) are noted. **J**, ALS spinal cord, severely degenerated hNSCs (GFP) exhibit HNE immuno-labeling (arrowheads). A larger grafted cell shows no 4-HNE damage (arrow). Scale bars = 50 μ m.

ALS microglia and astrocytes are not conducive to long-term survival of hNSC-derived motor neurons in vitro

To determine whether microglia and/or astrocytes were harmful to hNSC-derived motor neurons, direct contact cocultures were performed

between differentiated hNSCs and mixed glial cell populations. Primed and differentiated hNSCs were seeded on top of primary astrocytes and microglia isolated from normal rats (Figure 3A), astrocytes from normal rats and microglia from ALS rats post-disease onset (Figure 3B), and astrocytes and microglia from ALS rats (Figure 3C). Since Hb9 is a transcription factor specific for both premature and mature spinal motor neurons and MAP2 is a pan-marker for all mature neurons, spinal motor neurons *in vitro* were defined as Hb9⁺/MAP2⁺ cells. The survival of Hb9⁺/MAP2⁺ cells after one week in coculture was high in the presence of normal astrocytes and microglia (Figure 3A, D). Noticeably, many Hb9⁺ cells did not colabel with MAP2, indicating that they were in the early stage of motor neuron differentiation. The double-labeled cells displayed typical motor neuron morphology with multiple neurites (Figure 3A, insets). Replacing normal microglia with ALS microglia resulted in a 48% decrease in survival (Figure 3B, D). The presence of both ALS microglia and astroglia caused the greatest reduction (77% decrease) in Hb9⁺/MAP2⁺ cell survival (Figure 3C, D). Furthermore, Hb9⁺/MAP2⁺ cells exhibited morphology more characteristic of spinal motor neurons *in vivo* when cocultured with normal astrocytes and microglia (Figure 3A) compared to cocultures with ALS glial cells (Figure 3B, C). Microglia isolated from normal (Figure 3E) and ALS rats (Figure 3F) eleven days post-isolation in culture medium containing 7.5% serum were near pure (98%) and expressed Iba1, a pan-microglial marker for a calcium binding protein. Qualitative differences were not observed in CD11b (Figure 3E, F), a marker of resting microglia, and in CD68 (data not shown), a marker of activated microglia, through immunofluorescent staining analyses. Primary astroglia populations were not quite as pure (94% by GFAP immunostaining), and admixed with microglia (data not shown).

ALS microglia are specifically toxic to hNSC-derived motor neurons through nitroxidative stress

In order to determine whether ALS microglia were toxic to hNSC-derived motor neurons, cocultures were performed in direct contact in N2 media with differentiated hNSCs seeded on top of primary microglia. After 7 days of coculture, immunofluorescent staining with the Iba1 antibody was performed to detect either normal or

ALS microglia. When cocultured with hNSC-derived motor neurons, most normal microglia exhibited a ramified morphology indicative of a resting state (Figure 4A), whereas most ALS microglia displayed an activated/phagocytic morphology (Figure 4B). The total number of cells was also reduced in cocultures with ALS microglia as shown by DAPI staining in the merged images, indicating increased cell death. Immunofluorescent staining with the Hb9 motor neuron marker and MAP2 neuronal marker in coculture with normal (Figure 4C) and ALS (Figure 4D) rat microglia is also shown. Reduced immuno-labeled cell numbers and probable phagocytic microglia, which showed intense Hb9 and MAP2 staining, were observed in cocultures with ALS microglia (Figure 4D). Furthermore, representative images of TUNEL staining for apoptotic cell death are shown in normal (Figure 4E) and ALS (Figure 4F) microglia cocultures. Increased TUNEL staining and reduced total cell number were observed in cocultures with ALS microglia (Figure 4F). Cumulative data of direct contact cocultures showed that ALS microglia significantly reduced the numbers of Hb9⁺/MAP2⁺ cells (56% decrease) (Figure 4G) and increased the percentage of TUNEL positive cells (6.4-fold increase) (Figure 4H). Further controls included differentiated hNSCs only in N2 medium as well as cocultures with microglia isolated from 1 month old presymptomatic ALS rats and normal rats, which showed no differences among groups (Figure 4G-H).

Although the presence of increased oxidative and nitrosative damage in the degenerating areas of the spinal cord and motor cortex in ALS is indisputable, the exact source of reactive oxygen and nitrogen species is ambiguous. Given that many hNSCs showed damage consisting of protein nitration and lipid peroxidation at the disease end-stage in the spinal cords of ALS rats, we aimed to test whether microglia from ALS rats post-disease onset could potentially contribute to nitroxidative damage to hNSC-derived motor neurons. Furthermore, initial trial experiments revealed that ALS microglia-mediated neurotoxicity required direct contact between microglia and hNSC-derived motor neurons, indicating that the toxic factors generated from microglia are short-lived. Additionally, toxic effects were not observed when cocultures were performed in culture medium containing serum or B27 medium, which contains a variety of antioxidants, hormones and other pro-

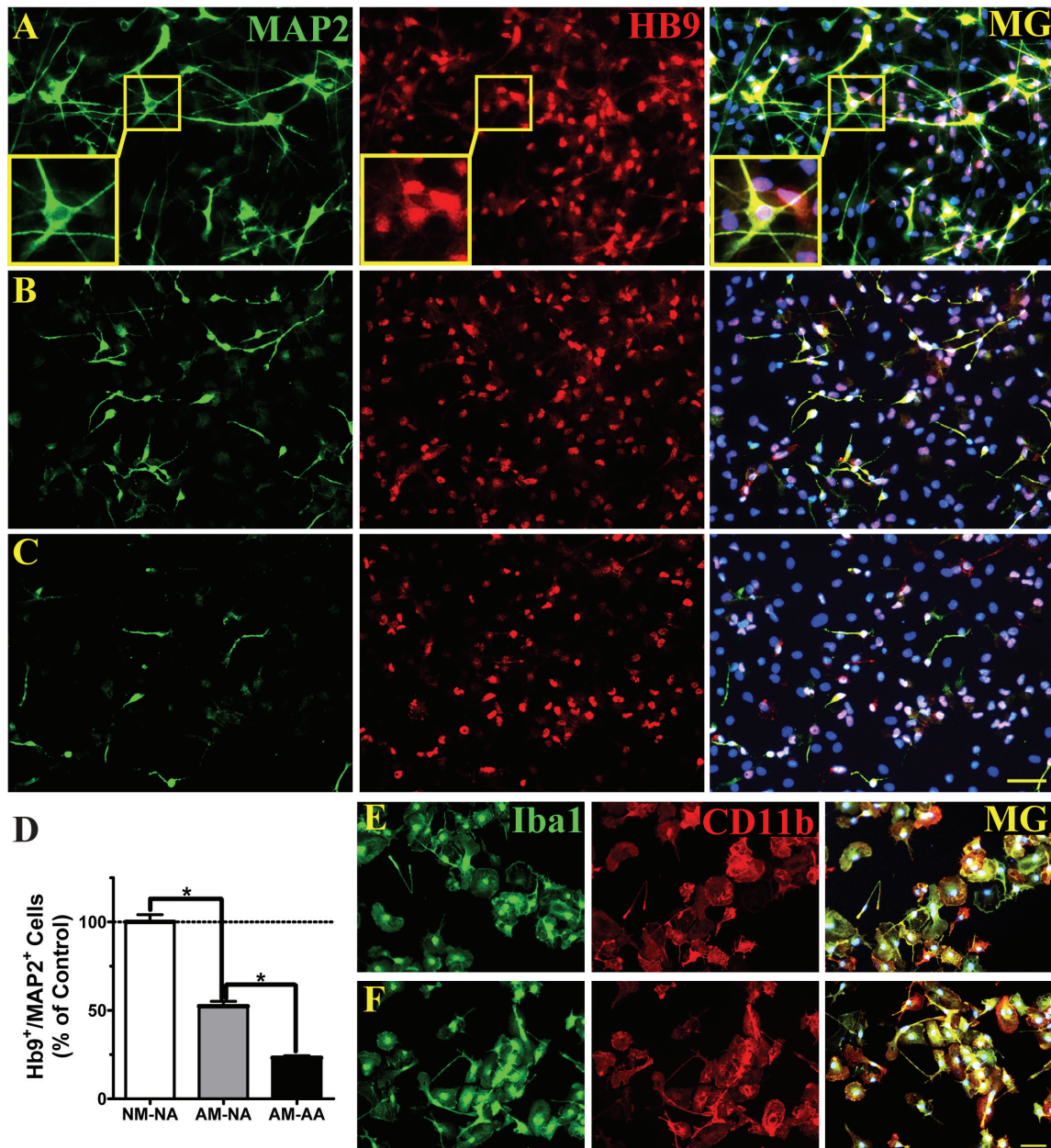


Figure 3. ALS microglia and astrocytes do not support survival of hNSC-derived motor neurons *in vitro*. Human NSC-derived motor neurons, expressing microtubule associated protein 2 (MAP2, green, neuronal marker) and Hb9 (red, motor neuron transcription factor), were cocultured in direct contact with both microglia and astrocytes. Merged imaged with DAPI shown in blue (MG). **A**, Normal microglia and normal astrocytes. Insets show magnified images of an Hb9⁺/MAP2⁺ motor neuron. **B**, ALS microglia and normal astrocytes. **C**, ALS microglia and ALS astrocytes. **D**, Average relative percentages of Hb9⁺/MAP2⁺ cells in each group (NA = normal adult astrocytes, NM = normal adult microglia, AA = post-disease onset ALS astrocytes and AM = post-disease onset ALS microglia). Data expressed as mean \pm SEM (n = 3, *p < 0.05 by one-way ANOVA with post-hoc Tukey test). **E**, Normal microglia express Iba1 (pan-microglia marker, green) and CD11b (resting microglia marker, red). **F**, ALS microglia express Iba1 and CD11b. **A-C** and **E-F**, scale bars = 50 μ m.

survival factors (data not shown). All these findings indicated the necessity to investigate the

role of short-lived free radicals in microglia-mediated toxicity. Along this line, expression

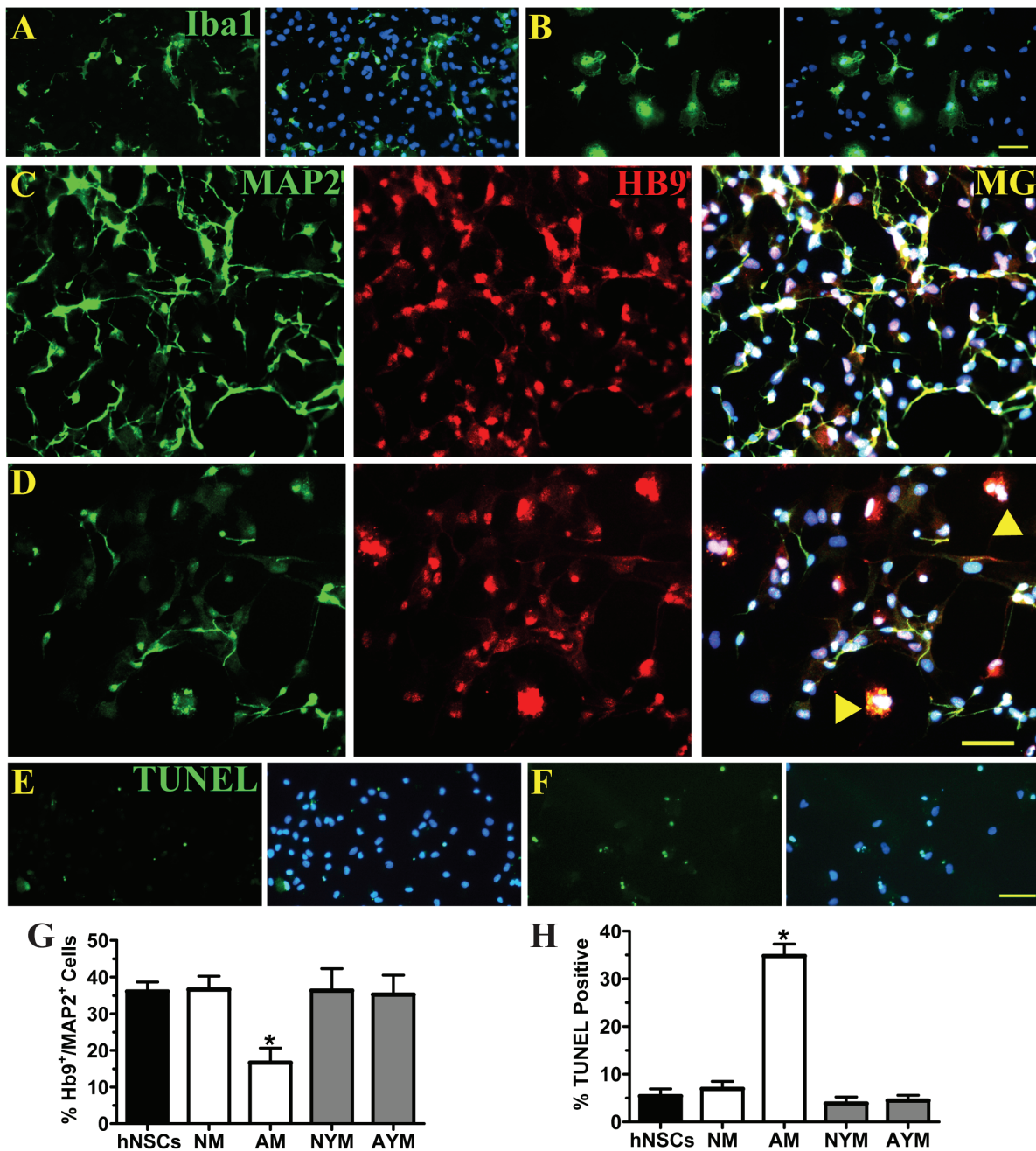


Figure 4. ALS microglia are toxic to hNSC-derived motor neurons. **A**, Normal microglia (Iba1, green) in direct contact coculture with hNSCs (DAPI, blue). **B**, ALS microglia post-disease onset (Iba1, green) in coculture with hNSCs (DAPI, blue). Note the difference in morphology between normal and ALS microglia. **C**, Human NSC-derived motor neurons, expressing microtubule associated protein 2 (MAP2, green, neuronal marker) and Hb9 (red, motor neuron transcription factor), cocultured with normal microglia. Merged image with DAPI shown in blue (MG). **D**, Human NSC-derived motor neurons (Hb9⁺/MAP2⁺) cocultured with ALS microglia. Presumably phagocytic/activated microglia shown by arrowheads. **E**, Apoptotic, TUNEL positive (green) cells in cocultures between normal microglia and hNSCs (DAPI, blue). **F**, TUNEL positive cells in cocultures between ALS microglia and hNSCs. **G**, Average percentages of Hb9⁺/MAP2⁺ cells in each group. **H**, Average percentages of TUNEL positive cells in each group. **A-F**, scale bars = 50 μ m. **G-H**, Data expressed as mean \pm SEM (n = 3). Human NSCs only (hNSCs), normal adult microglia (NM), post-disease onset ALS microglia (AM), normal young (1 month) microglia (NYM) and ALS young (1 month) microglia (AYM). *p < 0.05, significantly different from hNSCs group by one-way ANOVA with post-hoc Dunnett test.

levels of crucial enzymes relevant to nitric oxide and superoxide production were first characterized through immunofluorescent staining. Normal microglia expressed lower levels of inducible nitric oxide synthase (iNOS) and gp91^{phox} (Figure 5A), the catalytic subunit of NADPH oxidase, than ALS microglia isolated after disease onset (Figure 5B). Furthermore, after coculture with differentiated hNSCs for 7 days, microglia from normal adult rats induced a slight increase in lipid peroxidation as shown by brownish immunostaining with the 4-HNE adduct (Figure 5C). Cocultures with ALS microglia after disease onset caused more cell loss and small, dark brown cells indicative of increased cell death and lipid peroxidation (Figure 5D). In contrast, hNSC-derived motor neurons, when cocultured with normal (Figure 5E) or ALS (Figure 5F) microglia from 1 month old rats, showed no apparent lipid peroxidation.

Additionally, ALS microglia isolated after disease onset produced more nitric oxide (33% increase) (Figure 5G) and superoxide (46% increase) (Figure 5H) than normal adult microglia. In accordance with the increased 4-HNE staining in normal adult microglia cocultures, microglia isolated from 1 month old rats generated significantly less nitric oxide (normal, 65% decrease; ALS, 55% decrease) and superoxide (normal, 93% decrease; ALS, 93% decrease) than normal adult microglia. Selectively inhibiting NADPH oxidase and iNOS with apocynin (100 μ M) and L-NIL (100 μ M), respectively, throughout the duration of the coculture partially ameliorated Hb9⁺/MAP2⁺ cell loss (apocynin, 43% increase; L-NIL, 49% increase) (Figure 5I) and significantly reduced the number of TUNEL positive apoptotic cells (apocynin, 47% decrease; L-NIL, 46% decrease) (Figure 5J). Scavengers for peroxynitrite (urate-100 μ M), nitric oxide (carboxy-PTIO-20 μ M) and superoxide (SOD-100 U/ml) also provided partial protection to Hb9⁺/MAP2⁺ cells (urate, 39% increase; c-PTIO, 31% increase; SOD, 29% increase) in coculture with ALS microglia (Figure 5I).

ALS astrocytes lose neuroprotective capacity and exhibit toxicity to hNSC-derived motor neurons

Recent evidence has shown that either direct contact cocultures with primary astrocytes isolated from neonatal transgenic ALS mice, or

conditioned media from these cells, is toxic to embryonic stem cell-derived motor neurons [16-19]. We have previously shown that normal adult astroglia conditioned medium and cocultures maintain long-term survival of hNSC-derived motor neurons, and that the secretion of bFGF from astrocytes was partially responsible for neuroprotection *in vitro* [29]. To determine whether ALS astrocytes lose this protective capacity, primary astroglia were seeded in transwells and cocultured with differentiated hNSCs. These cocultures were non-contact in nature, as the transwell bottoms were positioned 1 mm above the hNSCs, which were attached to glass cover slips. After 7 days in coculture in N2 medium, normal astroglia derived from both adult and 1 month old rats provided significant long-term protection for Hb9⁺/MAP2⁺ cells (adult, 20% increase; 1 month, 28% increase) (Figure 6A). On the other hand, astroglia isolated from ALS rats did not display this same neuroprotective capacity and in fact, exhibited significant toxicity. Further, ALS astrocytes isolated after disease onset caused a greater decrease in the percentage of Hb9⁺/MAP2⁺ cells than astrocytes isolated from 1 month old ALS rats (disease onset, 47% decrease; 1 month, 24% decrease) (Figure 6A). Non-contact cocultures with ALS astroglia isolated after disease onset also resulted in a higher percentage of TUNEL positive cells (5.2-fold increase) than the differentiated hNSC only population (Figure 6B). Additionally, prostaglandin D2 (PGD2) has been implicated in transgenic ALS astrocyte-mediated toxicity to embryonic stem cell-derived motor neurons [18]. Indeed, ALS astrocytes isolated after disease onset released significantly higher levels of PGD2 as detected by PGD2 ELISA (54% increase) (Figure 6C). Selectively inhibiting the PGD2 receptor with MK 0524 (10 μ M) in non-contact cocultures with post-disease onset ALS astroglia partially prevented hNSC-derived motor neuron loss after 7 days (Figure 6D). However, the direct exposure of hNSC-derived motor neurons to exogenous PGD2 at concentrations equal or higher than 1 nM (350 μ g/ml), the approximate amount of PGD2 secreted from ALS microglia and normal astrocyte cocultures, did not cause significant toxicity (Figure 6E).

ALS microglia induce a loss in the neuroprotective capacity of normal astrocytes

Interactions between microglia, astrocytes and motor neurons within the diseased setting in

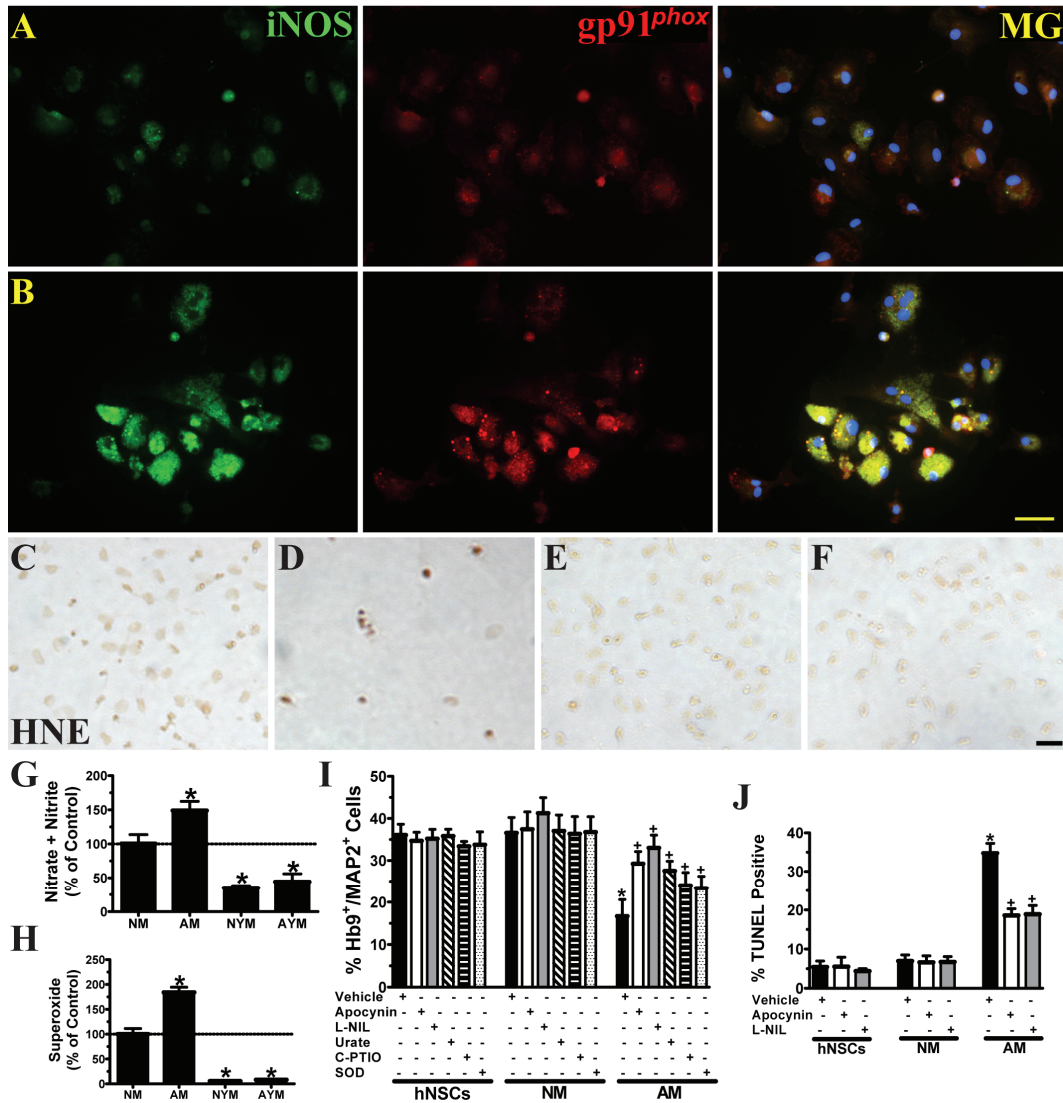


Figure 5. ALS microglia are detrimental to hNSC-derived motor neurons through nitrooxidative stress. **A**, Normal microglia express lower levels of enzymes that produce nitric oxide and superoxide, including inducible Nitric Oxide Synthase (iNOS, green) and gp91^{phox} (catalytic subunit of NADPH oxidase, red), respectively. Merged image with DAPI shown in blue (MG). **B**, ALS microglia post-disease onset express much higher levels of iNOS and gp91^{phox}. **C**, Normal adult microglia slightly increase lipid peroxidation (HNE) in direct contact coculture with hNSCs. **D**, ALS microglia post-disease onset dramatically increase lipid peroxidation. **E**, Normal young (1 month) microglia cause no observable lipid peroxidation. **F**, ALS young (1 month) microglia cause no observable lipid peroxidation. **G**, Relative average amounts of nitric oxide released into the medium (n = 3-4). *p < 0.05, significantly different from the NM group by one-way ANOVA with post-hoc Dunnett test. **H**, Relative average amounts of superoxide released into the medium (n = 3-5). *p < 0.05, significantly different from the NM group by one-way ANOVA with post-hoc Dunnett test. **I**, Average percentages of Hb9⁺/MAP2⁺ cells in each group treated with vehicle (DMSO and dH₂O are combined; hNSCs, n = 5; NM, n = 9; AM, n = 10); an NADPH oxidase inhibitor, apocynin (n = 3); an iNOS inhibitor, L-NIL (n = 3); a peroxynitrite scavenger, urate (n = 3); a nitric oxide scavenger, c-PTIO (n = 3); and a superoxide scavenger, SOD (n = 3). *p < 0.05, significantly different from hNSCs with vehicle group by one-way ANOVA with post-hoc Dunnett test. *p < 0.05, significantly different from AM with vehicle group by one-way ANOVA with post-hoc Dunnett test. **J**, Average percentages of TUNEL positive cells in each group treated with vehicle (DMSO and dH₂O are combined; hNSCs, n = 6; NM, n = 8; AM, n = 8); a NADPH oxidase inhibitor, apocynin (n = 3); and an iNOS inhibitor, L-NIL (n = 3). *p < 0.05, significantly different from hNSCs with vehicle group by one-way ANOVA with post-hoc Dunnett test. *p < 0.05, significantly different from AM with vehicle group by one-way ANOVA with post-hoc Dunnett test. **A-F**, scale bars = 50 μm. **G-J**, Data expressed as mean ± SEM. Human NSCs only (hNSCs), normal adult microglia (NM), post-disease onset ALS microglia (AM), normal young (1 month) microglia (NYM) and ALS young (1 month) microglia (AYM).

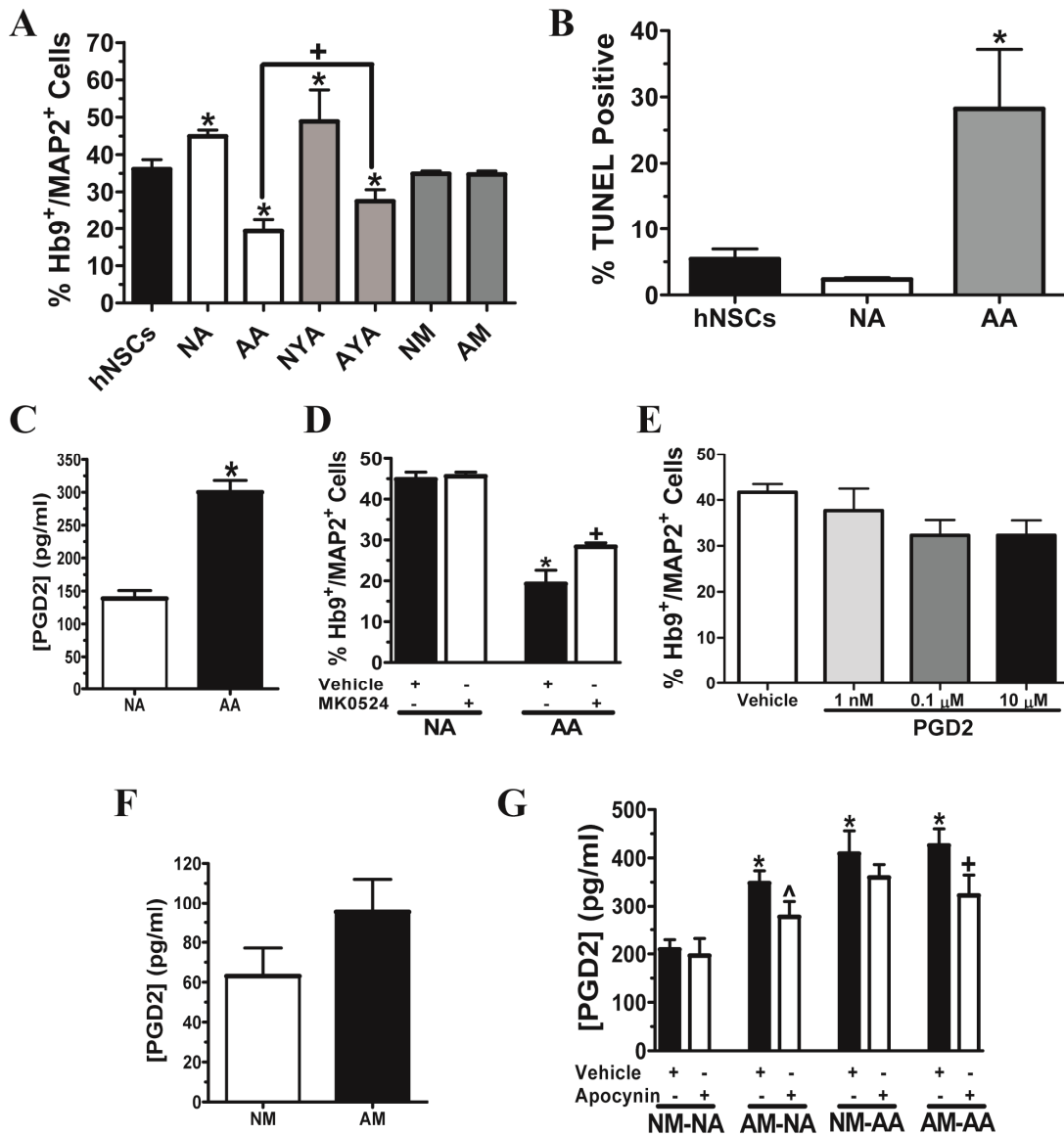


Figure 6. Prostaglandin D2 promotes ALS astroglia-mediated neurotoxicity. **A**, Average percentages of Hb9⁺/MAP2⁺ cells in each group of hNSCs in non-contact coculture (in transwells) with astrocytes or microglia (hNSCs, n = 5; NA and AA, n = 6; all other groups, n = 3). *p < 0.05, significantly different from hNSCs group, and +p < 0.05, significantly different between two groups, by one-way ANOVA with post-hoc Tukey test. **B**, Average percentages of TUNEL positive cells in each group of hNSCs in non-contact coculture with astrocytes (hNSCs, n = 6; NA and AA, n = 3). *p < 0.05, significantly different from hNSCs group by one-way ANOVA with post-hoc Dunnett test. **C**, PGD2 release into the medium from astrocytes (n = 6). *p < 0.05, significantly different from NA group by Student's t-test. **D**, Average percentages of Hb9⁺/MAP2⁺ cells in each group treated with vehicle (n = 6) or MK 0524 (n = 3), a PGD2 receptor inhibitor. *p < 0.05, significantly different from NA with vehicle group by Student's t-test. +p < 0.05, significantly different from AA with vehicle group by Student's t-test. **E**, Average percentages of Hb9⁺/MAP2⁺ cells in differentiated hNSCs treated with vehicle (DMSO, n = 3) or PGD2 (n = 3). Data analyzed by one-way ANOVA with post-hoc Tukey test. **F**, PGD2 release into the medium from microglia (n = 6). Data analyzed by Student's t-test. **G**, PGD2 release into the medium from astrocytes and microglia in direct contact coculture treated with vehicle (n = 6) or NADPH oxidase inhibitor, apocynin (n = 6). *p < 0.05, significantly different from NM-NA with vehicle group by one-way ANOVA with post-hoc Dunnett test. ^p = 0.0605, compared to AM-NA with vehicle group, and +p < 0.05, significantly different from AM-AA with vehicle group, by Student's t-test. **A-G**, Data expressed as mean ± SEM. Human NSCs only (hNSCs), normal adult astrocytes (NA), post-disease onset ALS astrocytes (AA), normal young (1 month) astrocytes (NYA), ALS young (1 month) astrocytes (AYA), normal adult microglia (NM) and post-disease onset ALS microglia (AM).

ALS have not been well characterized. Thus, we aimed to determine whether ALS microglia isolated after disease onset diminish the neuroprotective capacity of normal astrocytes and enhance the toxicity of ALS astrocytes to hNSC-derived motor neurons. The experimental design for the following experiments (**Figure 6-8**) consisted of a direct contact coculture between microglia and astrocytes by seeding them together in transwells (0.4 μm pore size) for 24 hrs prior to being positioned 1 mm above and cocultured with differentiated hNSCs that were located on glass coverslips at the bottom of the wells. Microglia were not observed on glass cover slips after being placed in transwells with the smaller pore size. Neither normal nor ALS microglia exhibited toxicity when independently placed in a transwell and cocultured in non-contact with differentiated hNSCs (**Figure 6A**). Microglia isolated from normal and ALS rats also released PGD2, but the levels were not significantly different (**Figure 6F**). However, when ALS microglia were cocultured in direct contact with normal adult astroglia for 7 days in N2 medium, a significant upregulation in PGD2 release was observed (40% increase) (**Figure 6G**). Furthermore, inhibiting NADPH oxidase with apocynin throughout the duration of the ALS microglia and normal astrocytes coculture resulted in a trend toward ameliorating the rise in PGD2 release ($p = 0.0605$). Inhibition of NADPH oxidase did, however, significantly reduce the amount of PGD2 release in cocultures with ALS microglia and ALS astrocytes (16% decrease) (**Figure 6G**). ALS microglia did not significantly enhance PGD2 release in cocultures with ALS astrocytes compared to cocultures between normal microglia and ALS astrocytes (**Figure 6G**).

To directly determine the effect of ALS microglia on the neuroprotective capacity of normal and ALS astrocytes, the survival of hNSC-derived motor neurons was evaluated after 7 days in non-contact coculture. Normal microglia and normal astrocytes maintained the survival of Hb9⁺/MAP2⁺ cells (**Figure 7A, E**). However, replacing normal microglia with post-disease onset ALS microglia resulted in a loss of the neuroprotective capacity of normal astrocytes shown by a 34% decrease in Hb9⁺/MAP2⁺ cells (**Figure 7B, E**). Hb9⁺/MAP2⁺ cells were lost in all cocultures with ALS astrocytes irrespective to the presence of normal (54% decrease) (**Figure 7C, E**) or ALS (54% decrease) microglia (**Figure 7D,**

E), indicating that normal microglia did not diminish the observed toxicity of ALS astrocytes. Quantitative analyses showed that Hb9⁺/MAP2⁺ cells were maintained if inhibitors of NADPH oxidase (23% increase) or iNOS (21% increase) were added throughout the duration of the direct coculture between ALS microglia and normal astrocytes (**Figure 7E**). Conversely, NADPH oxidase and iNOS inhibitors had no effect on the toxicity exerted by ALS astrocytes to hNSC-derived motor neurons irrespective to the presence of microglial cells either from ALS or normal rats (**Figure 7E**).

Non-contact cocultures with normal microglia and normal astrocytes also demonstrated reduced percentages of TUNEL positive cells in the differentiated hNSC population (2.1-fold decrease) (**Figure 8A, E**) whereas cocultures with ALS microglia in combination with normal astrocytes resulted in an increase in TUNEL staining (2.7-fold increase) (**Figure 8B, E**) compared to differentiated hNSCs only (**Figure 6B**). Fewer cells and higher percentages of TUNEL positive cells were further observed in cocultures between ALS astrocytes and normal microglia (5.1-fold increase) (**Figure 8C, E**) or ALS microglia (5.0-fold increase) (**Figure 8D, E**) compared to differentiated hNSCs only (**Figure 6B**).

Discussion

The ultimate goal of stem cell therapy in ALS is to restore motor function and thus, relies on the fate of transplanted stem cell-derived motor neurons in the ALS spinal cord. Here, we show that grafted human fetal NSCs develop into cholinergic neurons in the spinal cord of transgenic ALS rats, and that the cord microenvironment is detrimental to stem cell-derived motor neurons. Regarding the source for the toxic milieu in ALS, we reveal that microglia derived after symptomatic disease onset generate increased levels of nitroxidative stress that causes human motor neuron apoptosis and ablates the protective function of astrocytes. These data suggest that reactive oxygen and nitrogen species released from overactivated microglia in ALS directly damage human motor neurons and reduce the neuroprotective capacities of astrocytes, collectively compromising motor neuron survival in ALS.

Due to the lack of effective treatments for ALS, stem cells have become the arising hope to re-

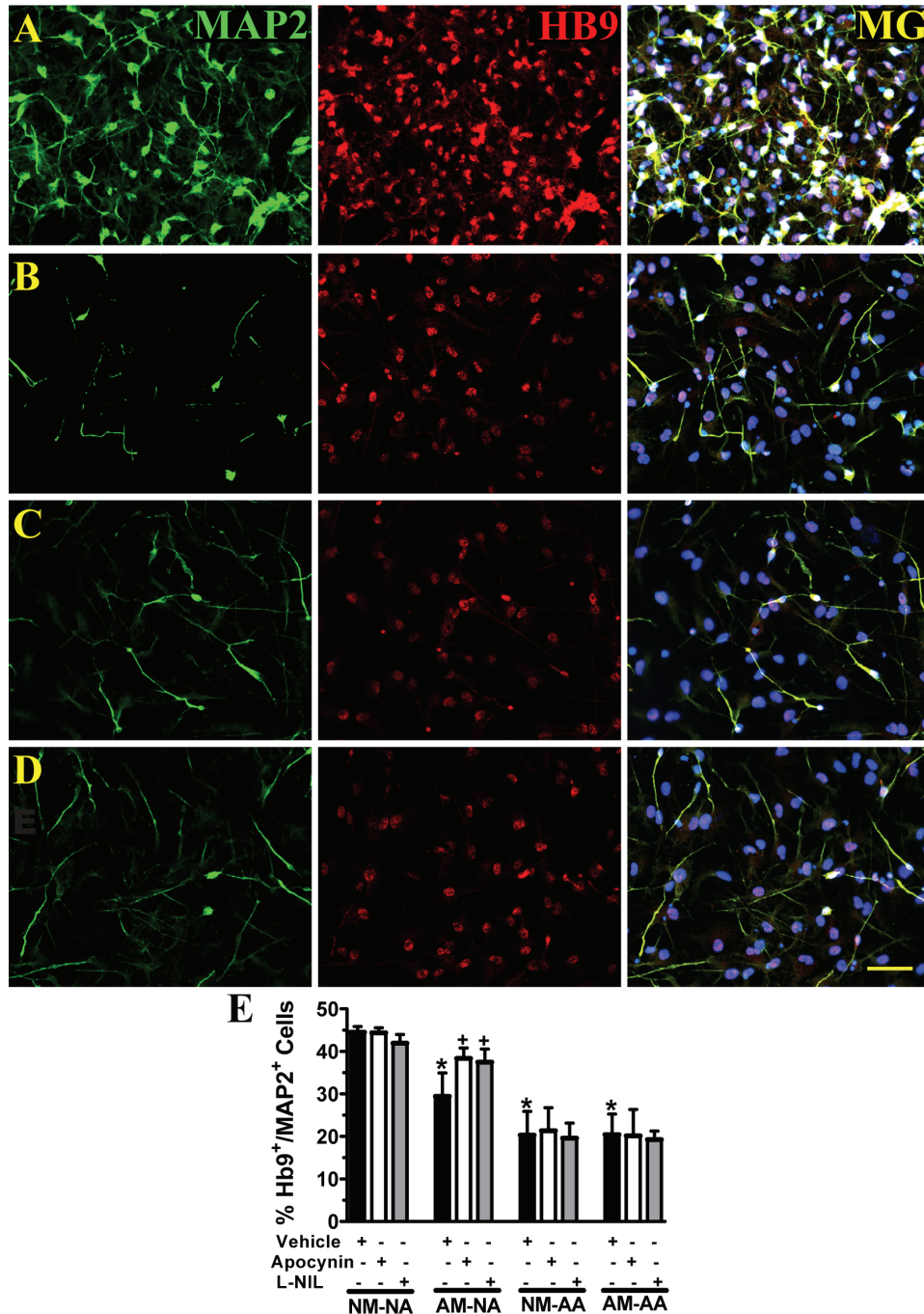


Figure 7. ALS microglia post-disease onset reduce the protective capacity of normal astrocytes resulting in the loss of hNSC-derived motor neurons. Microglia and astrocytes were cocultured together in transwells, and then in non-contact with hNSC-derived motor neurons, expressing microtubule associated protein 2 (MAP2, green, neuronal marker) and Hb9 (red, motor neuron transcription factor). Merged image with DAPI shown in blue (MG). **A**, Normal microglia and normal astrocytes. **B**, ALS microglia and normal astrocytes. **C**, Normal microglia and ALS astrocytes. **D**, ALS microglia and ALS astrocytes. **E**, Average percentages of Hb9⁺/MAP2⁺ cells in each group treated with vehicle (DMSO and dH₂O are combined, n = 6); NADPH oxidase inhibitor, apocynin (n = 3); and iNOS inhibitor, L-NIL (n = 3). *p < 0.05, significantly different from NM-NA with vehicle group by one-way ANOVA with post-hoc Dunnett test. ⁺p < 0.05, significantly different from AM-NA with vehicle group by one-way ANOVA with post-hoc Dunnett test. Data expressed as mean ± SEM. Normal adult microglia (NM), normal adult astrocytes (NA), post-disease onset ALS microglia (AM) and post-disease onset ALS astrocytes (AA). **A-D**, scale bar = 50 μm.

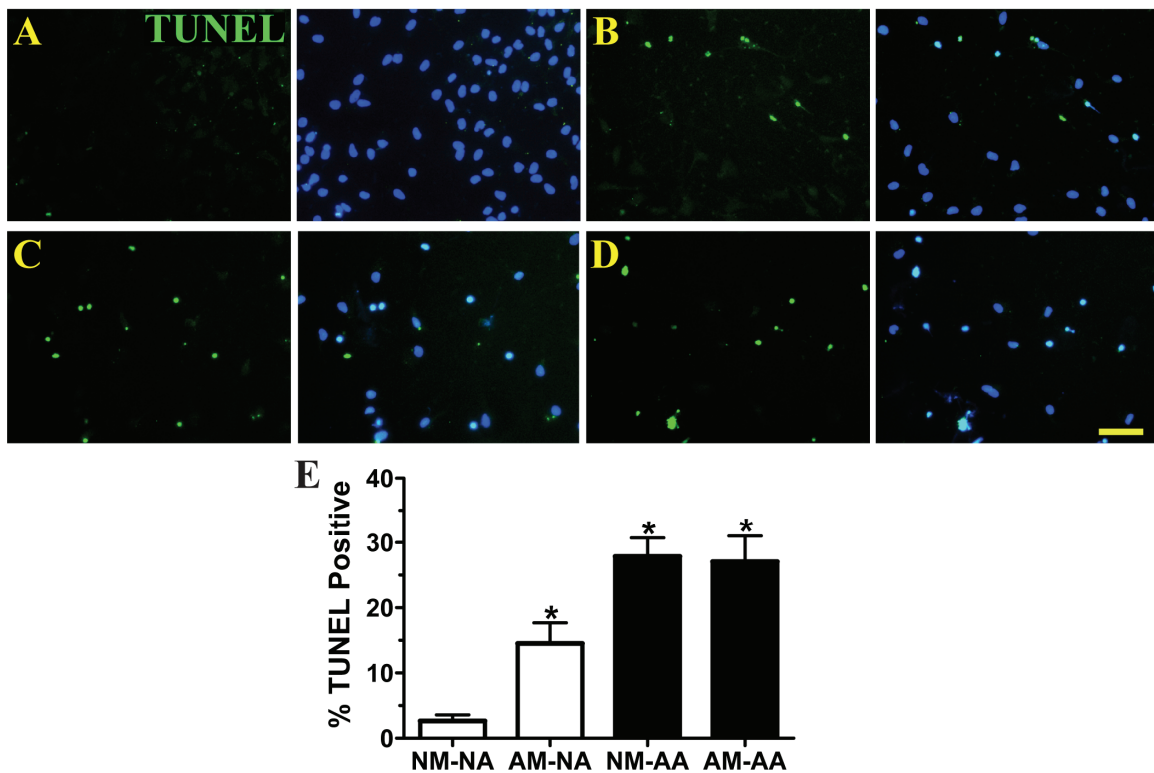


Figure 8. ALS microglia post-disease onset reduce the protective capacity of normal astrocytes resulting in hNSC-derived motor neuron apoptosis. Microglia and astrocytes were cocultured in transwells, and then in non-contact with hNSC-derived motor neurons. **A**, Apoptotic, TUNEL positive (green) cells in coculture with normal microglia and normal astrocytes. DAPI staining (blue) represents hNSC population. **B**, TUNEL positive cells in coculture with ALS microglia and normal astrocytes. **C**, TUNEL positive cells in coculture with normal microglia and ALS astrocytes. **D**, TUNEL positive cells in coculture with ALS microglia and ALS astrocytes. Note the decrease in total cell numbers in **B-D**. **E**, Average percentages of TUNEL positive cells in each group (n = 3). *p < 0.05, significantly different from NM-NA group by one-way ANOVA with post-hoc Dunnett test. Data expressed as mean \pm SEM. Normal adult microglia (NM), normal adult astrocytes (NA), post-disease onset ALS microglia (AM) and post-disease onset ALS astrocytes (AA). **A-D**, scale bar = 50 μ m.

place lost motor neurons. Stem cell transplants from different sources have been tested in transgenic ALS animal models [14], but only a few studies produced cholinergic cells [36,37]. We have previously shown that hNSCs differentiate into motor neurons *in vitro* and *in vivo* [21,23]. When grafted into spinal cords, hNSC-derived motor neuron axons reach the gastrocnemius muscle and improve motor function in motor neuron deficient rats [24,25]. However, the transplantation of hNSCs does not drastically delay disease progression or prolong lifespan in transgenic ALS rats (unpublished observation). Here, we report that the microenvironment in the spinal cord is unfavorable for human motor neurons possibly through increased nitroxidative damage. An earlier study found that grafted mouse olfactory bulb-neural

precursor cells differentiated into ChAT⁺ cells and extended processes into the sciatic nerve in transgenic ALS mice, but processes failed to reach distal muscle targets and a morphology indicating degenerating distal axons was observed [36]. In addition, mouse embryonic stem cell-derived motor neurons did not survive long-term in ALS rat spinal cords [37]. These results indicate that stem cell-derived motor neurons, like endogenous motor neurons, are susceptible to a hostile microenvironment in spinal cords of ALS. In these studies, stem cell-derived motor neurons were transplanted prior to symptomatic disease onset in which maturation occurred before drastic motor neuron toxicity developed. Thus, it remains unknown whether stem cell transplants could yield viable motor neurons when injected after disease onset, as would be

indicated in ALS patients.

In searching for potentially toxic sources to grafted hNSC-derived motor neurons in the ALS spinal cord, we turn to host astrocytes and microglia that are known to be critical in disease progression [2,4-6]. Previously, we have shown that normal adult astrocytes maintain the long-term survival of hNSC-derived motor neuron *in vitro* [29]. It was unknown whether ALS astrocytes would exhibit similar protective capacities for hNSC-derived motor neurons. Human embryonic stem cell-derived motor neurons have already been shown to be specifically vulnerable to neonatal ALS astrocyte-mediated toxicity [16,17]. In agreement with these studies, we show here that astrocytes isolated from transgenic ALS rats, especially after disease onset, lose neuroprotective capacity and exert additional toxicity to hNSC-derived motor neurons. In regards to the possible toxic factors released from ALS astrocytes, previous studies suggested that reactive nitrogen species (RNS) generated from ALS astrocytes promote motor neuronal death [38,39]. However, we found that ALS astrocytes did not require direct contact to elicit toxicity to hNSC-derived motor neurons, and that normal and ALS astroglia expressed similar levels of iNOS and released comparable levels of nitric oxide (unpublished observation). Thus, our study suggests that RNS may not play a direct role in ALS astroglia-mediated toxicity to hNSC-derived motor neurons, at least, *in vitro*. Other factors with relatively longer lifetimes may have been the main contributors to the observed neurotoxicity of ALS astroglia. On the other hand, a lack of release of protective/trophic factors from ALS astroglia, while simultaneously consuming limited nutrients from the medium, may have contributed to an increased rate of death of motor neurons *in vitro*. Along this line, we found that ALS and normal astrocytes cocultured with ALS microglia secreted abnormally high levels of PGD₂, but PGD₂ was not directly toxic to hNSC-derived motor neurons. All these findings are in agreement with a previous study suggesting that PGD₂ receptor activation in astrocytes may lead to motor neuron loss [18]. However, PGD₂ is likely not the only factor involved in ALS astrocyte-mediated toxicity, since blocking the PGD₂ receptor only partially protected hNSC-derived motor neurons. ALS astrocyte-induced motor neuron death possibly resulted from a combination of a decreased release of protective factors and an

increased release of toxic factors, which remain unknown and require further investigation.

In this study, we found that ALS microglia isolated after symptomatic disease onset contribute to human motor neuron toxicity through the increased production of reactive oxygen and nitrogen species (ROS/RNS), while those isolated at a presymptomatic stage (age 1 month) did not cause hNSC-derived motor neuron loss. The latter is different from previous reports showing that microglia isolated from neonatal transgenic ALS mice are toxic to primary embryonic rat motor neurons [6,40]. The discrepancy may be due to differences in the microglia isolation procedure, the type of motor neurons or the experimental design. Using density gradient centrifugation, we are able to obtain pure microglia in less than 4 days, which minimizes the possible artificial activation of the cells caused by *in vitro* culture for a longer period of time. Alternatively, the hNSC-derived motor neuron population contained approximately 30% GFAP⁺ cells [21], which may buffer the ALS microglia-mediated toxicity. The current study used a mixture of both spinal cord- and brain-derived microglia from ALS rats, and our preliminary studies indicated that they exhibited similar levels of toxicity to hNSC-derived motor neurons (unpublished observation). However, it is possible that microglia derived from the degenerating areas within the spinal cord may be more toxic, and thus, the *in vitro* model with mixed brain and spinal cord microglia may underestimate the toxic effects of ALS microglia on grafted human spinal motor neurons *in vivo*.

Our data, collected from a coculture system containing microglia, astrocytes and hNSC-derived motor neurons, suggest that ALS microglia derived after symptomatic disease onset exert damage by modifying normally neuroprotective astrocytes. Specifically, nitroxidative stress inflicts a loss in astrocytic capacity to protect motor neurons and causes increases in PGD₂ release. Our results suggest that stem cell-mediated astrocyte replacement may not sustain a beneficial effect, since the transplanted astrocytes may lose their neuroprotective phenotype when exposed to microglia within the ALS spinal cord. Further, it is known that ALS microglia and astrocytes display enhanced release of several proinflammatory factors [41,42] that may crosstalk and lead to a vicious cycle of exacerbated microglia overacti-

vation and astrocyte dysfunction. In an effort to explore potential mechanisms underlying harmful interactions between microglia and astrocytes, we examined the role of glutathione (GSH), the major antioxidant released from astrocytes, in hNSC-derived motor neuron protection. We found that ALS astrocytes exhibited inherent increased GSH synthesis and secretion *in vitro* compared to normal astrocytes, but GSH depletion in ALS astrocytes did not worsen ALS microglia-mediated toxicity to hNSC-derived motor neurons (unpublished observation). On the other hand, astroglia-mediated glutamate reuptake, which is known to be impaired in ALS [26,43], plays a critical role in promoting motor neuron death due to excitotoxicity. Furthermore, ROS/RNS inhibits glutamate uptake in astroglia cultures [44,45] and increases the susceptibility of motor neurons to glutamate-mediated toxicity [46]. Whether ALS microglia-generated nitroxidative stress directly interferes with the expression or function of the astroglial glutamate transporter, EAAT2, remains to be determined.

In conclusion, mutant SOD1-expressing microglia damage hNSC-derived motor neurons through enhanced release of ROS/RNS and direct nitroxidative damage. In addition, microglia-generated ROS/RNS, as well as other proinflammatory factors such as PGD2, lead to the inability of normal astrocytes to protect hNSC-derived motor neurons. The possibilities that mutant SOD1 astrocytes secrete factor(s) directly toxic to motor neurons and/or are unable to maintain a non-toxic level of glutamate also exist. Essentially, in order for stem cell treatments designed to replace spinal motor neurons to succeed and allow for motor function restoration in ALS patients, the harsh microenvironment within the spinal cord must first be drastically improved.

Acknowledgements

This investigation was supported by the National Institutes of Health under Ruth L. Kirschstein National Research Service Award (F30NS060387), the National Institutes of Health (NS046025), the TIRR Foundation, the Gillson Longenbaugh Foundation, the John S. Dunn Research Foundation, the Moody Foundation and the Cullen Foundation. The authors also thank Enyin Wang and Brandon Bassett for their technical assistance, as well as Dr. Stanley Appel and Dr. Richard Coggeshall for their critical reviews.

Please address correspondence to: Ping Wu, MD, PhD, Department of Neuroscience and Cell Biology, University of Texas Medical Branch, Galveston, TX 77555-0620, USA. Phone: 409-772-9858, Fax: 409-747-2200, E-mail: piwu@utmb.edu

References

- [1] Bruijn LI, Miller TM, and Cleveland DW. Unraveling the mechanisms involved in motor neuron degeneration in ALS. *Annu Rev Neurosci* 2004; 27: 723-749.
- [2] Boillee S, Yamanaka K, Lobsiger CS, Copeland NG, Jenkins NA, Kassiotis G, Kollias G, and Cleveland DW. Onset and progression in inherited ALS determined by motor neurons and microglia. *Science* 2006; 312(5778): 1389-1392.
- [3] Yamanaka K, Boillee S, Roberts EA, Garcia ML, McAlonis-Downes M, Mikse OR, Cleveland DW, and Goldstein LS. Mutant SOD1 in cell types other than motor neurons and oligodendrocytes accelerates onset of disease in ALS mice. *Proc Natl Acad Sci U S A* 2008; 105(21): 7594-7599.
- [4] Clement AM, Nguyen MD, Roberts EA, Garcia ML, Boillee S, Rule M, McMahan AP, Doucette W, Siwek D, Ferrante RJ, Brown RH, Jr., Julien JP, Goldstein LS, and Cleveland DW. Wild-type nonneuronal cells extend survival of SOD1 mutant motor neurons in ALS mice. *Science* 2003; 302(5642): 113-117.
- [5] Yamanaka K, Chun SJ, Boillee S, Fujimori-Tonou N, Yamashita H, Gutmann DH, Takahashi R, Misawa H, and Cleveland DW. Astrocytes as determinants of disease progression in inherited amyotrophic lateral sclerosis. *Nat Neurosci* 2008; 11(3): 251-253.
- [6] Beers DR, Henkel JS, Xiao Q, Zhao W, Wang J, Yen AA, Siklos L, McKercher SR, and Appel SH. Wild-type microglia extend survival in PU.1 knockout mice with familial amyotrophic lateral sclerosis. *Proc Natl Acad Sci U S A* 2006; 103(43): 16021-16026.
- [7] Kawamata T, Akiyama H, Yamada T, and McGeer PL. Immunologic reactions in amyotrophic lateral sclerosis brain and spinal cord tissue. *Am J Pathol* 1992; 140(3): 691-707.
- [8] Schiffer D, Cordera S, Cavalla P, and Migheli A. Reactive astrogliosis of the spinal cord in amyotrophic lateral sclerosis. *J Neurol Sci* 1996; 139 Suppl: 27-33.
- [9] Shaw PJ, Ince PG, Falkous G, and Mantle D. Oxidative damage to protein in sporadic motor neuron disease spinal cord. *Ann Neurol* 1995; 38(4): 691-695.
- [10] Beal MF, Ferrante RJ, Browne SE, Matthews RT, Kowall NW, and Brown RH, Jr. Increased 3-nitrotyrosine in both sporadic and familial amyotrophic lateral sclerosis. *Ann Neurol* 1997; 42(4): 644-654.
- [11] Smith RG, Henry YK, Mattson MP, and Appel

- SH. Presence of 4-hydroxynonenal in cerebrospinal fluid of patients with sporadic amyotrophic lateral sclerosis. *Ann Neurol* 1998; 44(4): 696-699.
- [12] Nayak MS, Kim YS, Goldman M, Keirstead HS, and Kerr DA. Cellular therapies in motor neuron diseases. *Biochim Biophys Acta* 2006; 1762(11-12): 1128-1138.
- [13] Hedlund E, Hefferan MP, Marsala M, and Isaacson O. Cell therapy and stem cells in animal models of motor neuron disorders. *Eur J Neurosci* 2007; 26(7): 1721-1737.
- [14] Thonhoff JR, Ojeda LD, and Wu P. Stem cell-derived motor neurons: applications and challenges in amyotrophic lateral sclerosis. *Current Stem Cell Research and Therapy* 2009; 4(3): 178-199.
- [15] Kim YS, Martinez T, Deshpande DM, Drummond J, Provost-Javier K, Williams A, McGurk J, Maragakis N, Song H, Ming GL, and Kerr DA. Correction of humoral derangements from mutant superoxide dismutase 1 spinal cord. *Ann Neurol* 2006; 60(6): 716-728.
- [16] Nagai M, Re DB, Nagata T, Chalazonitis A, Jessell TM, Wichterle H, and Przedborski S. Astrocytes expressing ALS-linked mutated SOD1 release factors selectively toxic to motor neurons. *Nat Neurosci* 2007; 10(5): 615-622.
- [17] Di Giorgio FP, Carrasco MA, Siao MC, Maniatis T, and Eggan K. Non-cell autonomous effect of glia on motor neurons in an embryonic stem cell-based ALS model. *Nat Neurosci* 2007; 10(5): 608-614.
- [18] Di Giorgio FP, Boulting GL, Bobrowicz S, and Eggan KC. Human embryonic stem cell-derived motor neurons are sensitive to the toxic effect of glial cells carrying an ALS-causing mutation. *Cell Stem Cell* 2008; 3(6): 637-648.
- [19] Marchetto MC, Muotri AR, Mu Y, Smith AM, Cezar GG, and Gage FH. Non-cell-autonomous effect of human SOD1 G37R astrocytes on motor neurons derived from human embryonic stem cells. *Cell Stem Cell* 2008; 3(6): 649-657.
- [20] Tarasenko YI, Yu YJ, Jordan PM, Bottenstein J, and Wu P. Effect of growth factors on proliferation and phenotypic differentiation of human fetal neural stem cells. *Journal of Neuroscience Research* 2004; 78(5): 625-636.
- [21] Jordan PM, Ojeda LD, Thonhoff JR, Gao JL, Boehning D, Yu YJ, and Wu P. Generation of Spinal Motor Neurons From Human Fetal Brain-Derived Neural Stem Cells: Role of Basic Fibroblast Growth Factor. *Journal of Neuroscience Research* 2009; 87(2): 318-332.
- [22] Bottenstein JE and Sato GH. Growth of A Rat Neuroblastoma Cell Line in Serum-Free Supplemented Medium. *Proceedings of the National Academy of Sciences of the United States of America* 1979; 76(1): 514-517.
- [23] Wu P, Tarasenko YI, Gu Y, Huang LY, Coggeshall RE, and Yu Y. Region-specific generation of cholinergic neurons from fetal human neural stem cells grafted in adult rat. *Nat Neurosci* 2002; 5(12): 1271-1278.
- [24] Gao J, Coggeshall RE, Tarasenko YI, and Wu P. Human neural stem cell-derived cholinergic neurons innervate muscle in motoneuron deficient adult rats. *Neuroscience* 2005; 131(2): 257-262.
- [25] Gao J, Coggeshall RE, Chung JM, Wang J, and Wu P. Functional motoneurons develop from human neural stem cell transplants in adult rats. *Neuroreport* 2007; 18(6): 565-569.
- [26] Howland DS, Liu J, She Y, Goad B, Maragakis NJ, Kim B, Erickson J, Kulik J, DeVito L, Psaltis G, DeGennaro LJ, Cleveland DW, and Rothstein JD. Focal loss of the glutamate transporter EAAT2 in a transgenic rat model of SOD1 mutant-mediated amyotrophic lateral sclerosis (ALS). *Proc Natl Acad Sci U S A* 2002; 99(3): 1604-1609.
- [27] Thonhoff JR, Jordan PA, Karam JR, Bassett BL, and Wu P. Identification of early disease progression in an ALS rat model. *Neuroscience Letters* 2007; 415(3): 264-268.
- [28] Schwartz JP and Wilson DJ. Preparation and Characterization of Type-1 Astrocytes Cultured from Adult-Rat Cortex, Cerebellum, and Striatum. *Glia* 1992; 5(1): 75-80.
- [29] Jordan PM, Cain LD, and Wu P. Astrocytes enhance long-term survival of cholinergic neurons differentiated from human fetal neural stem cells. *Journal of Neuroscience Research* 2008; 86(1): 35-47.
- [30] Saura J, Tusell JM, and Serratos J. High-yield isolation of murine microglia by mild trypsinization. *Glia* 2003; 44(3): 183-189.
- [31] Frank MG, Wieseler-Frank JL, Watkins LR, and Maier SF. Rapid isolation of highly enriched and quiescent microglia from adult rat hippocampus: Immunophenotypic and functional characteristics. *Journal of Neuroscience Methods* 2006; 151(2): 121-130.
- [32] Pang ZJ, Chen Y, and Zhou M. L929 cell conditioned medium protects RAW264.7 cells from oxidative injury through inducing antioxidant enzymes. *Cytokine* 2000; 12(7): 944-950.
- [33] Ponomarev ED, Novikova M, Maresz K, Shriver LP, and Dittel BN. Development of a culture system that supports adult microglial cell proliferation and maintenance in the resting state. *Journal of Immunological Methods* 2005; 300(1-2): 32-46.
- [34] Tan AS and Berridge MV. Superoxide produced by activated neutrophils efficiently reduces the tetrazolium salt, WST-1 to produce a soluble formazan: a simple colorimetric assay for measuring respiratory burst activation and for screening anti-inflammatory agents. *Journal of Immunological Methods* 2000; 238(1-2): 59-68.
- [35] Zhao WH, Beers DR, Henkel JS, Zhang W, Urushitani M, Julien JP, and Appel SH. Extracellular Mutant SOD1 Induces Microglial-Mediated

Glial interactions and toxicity to motoneurons

- Motoneuron Injury. *Glia* 2010; 58(2): 231-243.
- [36] Martin LJ and Liu Z. Adult olfactory bulb neural precursor cell grafts provide temporary protection from motor neuron degeneration, improve motor function, and extend survival in amyotrophic lateral sclerosis mice. *J Neuropathol Exp Neurol* 2007; 66(11): 1002-1018.
- [37] Lopez-Gonzalez R, Kunckles P, and Velasco I. Transient Recovery in a Rat Model of Familial Amyotrophic Lateral Sclerosis After Transplantation of Motor Neurons Derived From Mouse Embryonic Stem Cells. *Cell Transplantation* 2009; 18(10-11): 1171-1181.
- [38] Barbeito LH, Pehar M, Cassina P, Vargas MR, Peluffo H, Viera L, Estevez AG, and Beckman JS. A role for astrocytes in motor neuron loss in amyotrophic lateral sclerosis. *Brain Res Brain Res Rev* 2004; 47(1-3): 263-274.
- [39] Cassina P, Cassina A, Pehar M, Castellanos R, Gandelman M, de Leon A, Robinson KM, Mason RP, Beckman JS, Barbeito L, and Radi R. Mitochondrial dysfunction in SOD1G93A-bearing astrocytes promotes motor neuron degeneration: prevention by mitochondrial-targeted antioxidants. *J Neurosci* 2008; 28(16): 4115-4122.
- [40] Xiao Q, Zhao W, Beers DR, Yen AA, Xie W, Henkel JS, and Appel SH. Mutant SOD1(G93A) microglia are more neurotoxic relative to wild-type microglia. *J Neurochem* 2007; 102(6): 2008-2019.
- [41] Weydt P, Yuen EC, Ransom BR, and Moller T. Increased cytotoxic potential of microglia from ALS-transgenic mice. *Glia* 2004; 48(2): 179-182.
- [42] Hensley K, Abdel-Moaty H, Hunter J, Mhatre M, Mou S, Nguyen K, Potapova T, Pye QN, Qi M, Rice H, Stewart C, Stroukoff K, and West M. Primary glia expressing the G93A-SOD1 mutation present a neuroinflammatory phenotype and provide a cellular system for studies of glial inflammation. *J Neuroinflammation* 2006; 3: 2
- [43] Appel SH, Beers D, Siklos L, Engelhardt JI, and Mosier DR. Calcium: the Darth Vader of ALS. *Amyotroph Lateral Scler Other Motor Neuron Disord* 2001; 2 Suppl 1: S47-S54.
- [44] Rao SD, Yin HZ, and Weiss JH. Disruption of glial glutamate transport by reactive oxygen species produced in motor neurons. *Journal of Neuroscience* 2003; 23(7): 2627-2633.
- [45] Miralles VJ, Martinez-Lopez I, Zaragoza R, Borrás E, Garcia C, Pallardo FV, and Vina JR. Na⁺ dependent glutamate transporters (EAAT1, EAAT2, and EAAT3) in primary astrocyte cultures: effect of oxidative stress. *Brain Research* 2001; 922(1): 21-29.
- [46] Zhao W, Xie W, Le W, Beers DR, He Y, Henkel JS, Simpson EP, Yen AA, Xiao Q, and Appel SH. Activated microglia initiate motor neuron injury by a nitric oxide and glutamate-mediated mechanism. *J Neuropathol Exp Neurol* 2004; 63(9): 964-977.